Electronic Research Archive

http://www.aimspress.com/journal/era

ERA, 34(3): 1671–1690.
DOI: 10.3934/era.2026076
Received: 18 November 2025
Revised: 22 January 2026
Accepted: 30 January 2026
Published: 27 February 2026

Research article

Cooperative voltage regulation of unknown DC microgrids: A data-driven robust distributed control strategy

Yiwen Shi, Junjie Jiang, Xin Chen, Tiansheng Zhang, Shicheng Huo* **and Jianfei Yang***

School of Electrical and Automation Engineering, Nanjing Normal University, Nanjing 210023, China

* **Correspondence:** Email: shichenghuo123@njnu.edu.cn, yjfsmile@njnu.edu.cn.

Abstract: In this paper, a data-driven robust distributed control strategy is proposed for cooperative voltage regulation of the direct-current (DC) microgrids such that the output voltages of all distributed generation units (DGUs) track the specified reference signal. Unlike in decentralized control where all DGUs need to know the information of the reference signal, each DGU only needs to obtain the information of its neighbors in the proposed distributed control strategy. In the presence of the unknown parameters of DGUs, a data-driven robust control method is proposed to achieve cooperative voltage regulation under the available data affected by noise. It is shown that the cooperative voltage regulation problem can be transformed into a local stabilization problem based on the proposed distributed control protocol. To address the local stabilization problem, the noisy data from local DGU and the constructed auxiliary system is collected, and then we develop a data-driven control framework that guarantees robust closed-loop stability under bounded noise. We formulate a data-dependent linear matrix inequality (LMI) based on $\mathcal{D}_Q$-stabilization theory. This LMI enforces all eigenvalues of the closed-loop system to lie within a specified region inside the unit disk, thereby quantifying robustness through guaranteed stability margins when the collected data is corrupted by noise. The resulting gain matrices of the distributed control protocol are computed directly from noisy-data-dependent LMI without requiring any explicit model knowledge. Several simulation results are provided to show the effectiveness and robustness of the proposed methods.

Keywords: distributed control; robust control; data-driven control; DC microgrid; voltage regulation

1. Introduction

The direct-current (DC) microgrid is constructed by directly connecting distributed power sources, energy storage devices, and electrical loads, which form the autonomous systems that can connect to power grids or operate independently. The DC microgrid can be used to supply power to devices such as electric vehicles, mobile robots, and unmanned aerial vehicles [1–7]. In recent years, with the widespread application of the DC microgrid, several control strategies have been proposed. In [8, 9], the centralized control method was used for energy management and performance optimization of the DC microgrid. The centralized control method needs each distributed generation unit (DGU) to have information about all the other DGUs, which results in an increase in communication costs. To overcome this deficiency, the decentralized control method was employed in [10–12]. In [10], a decentralized secondary control method was proposed to achieve voltage restoration of the microgrid cluster system. In [11], an adaptive decentralized control method was designed to mitigate the influence of transfer impedance. In [12], a decentralized active disturbance rejection control method was introduced for hybrid energy storage system to eliminate the disturbance's impacts. The decentralized control avoids communication between DGUs, but it leads to a lack of collaboration among the DGUs. This results in the control of each DGU not being globally optimal.

Note that the decentralized control requires that all DGUs be able to directly receive the central reference instruction, which means that all DGUs need to communicate with the central unit. This situation also leads to an increase in communication costs. To avoid this problem, the distributed control method was proposed in [13–16], where only one or a few DGUs need to receive the central reference instruction. In [13], a distributed control method was presented to realize the optimal coordination between traditional generations and renewable generations in the DC microgrid. In [14], a distributed control protocol was designed to implement voltage regulation for the DC microgrid under various loads. In [15, 16], two types of secure distributed control methods were proposed for the networked DC microgrids subject to false data injection attacks. These distributed control protocols can achieve coordinated resource optimization and voltage regulation by constructing the sparse communication networks where each DGU only needs to obtain the information of its neighbors.

It is worth noting that the design of the aforementioned distributed control protocols in [13–16] is based on the precise parameters of DGUs in the DC microgrid. However, due to the complexity of actual working conditions and parameter uncertainties, it is difficult to obtain precise parameters of DGUs. Therefore, the data-driven control methods have been proposed to directly learn a feasible controller from measurable data. In [17], a data-driven distributed model predictive control control method was designed for voltage regulation of the DC microgrid under communication delays and packet dropouts. In [18], a data-driven reinforcement learning control approach was proposed to achieve voltage stability. In [19], a data-driven control algorithm based on machine learning was developed to enhance the robustness and response speed of the DC microgrid. In [20], a data-driven control method was designed to regulate the current interaction between the DC and alternating-current (AC) microgrids and control the terminal voltage of the DC microgrid. Although these data-driven control methods were designed, they all rely on intact measurement data. In reality, the noise is ubiquitous and can affect the authenticity of the measurement data. Therefore, it is worth studying how to design feasible control methods from data affected by noises, and this issue has rarely been discussed so far.

Based on the above analysis, this paper focuses on the cooperative voltage regulation issue for unknown DC microgrids via designing a data-driven robust distributed control method. The main contributions are as follows.

1) Compared with [13, 14, 17, 18] where the signal transmission among DGUs not only includes terminal voltage but also filter current, the distributed control protocol designed in this paper only

transmits terminal voltage data among DGUs. The advantage of the proposed method lies in the fact that it can avoid the configuration of the current sensor in signal interaction among DGUs.

2) Different from the data-driven control methods in [17–20], which consider the collected data in the noise-free environments, this paper considers that the collected data is affected by unknown noise. Then, a data-driven design method is proposed to design the feasible gain matrices of the distributed control protocol from the noisy data. Furthermore, we employ $\mathcal{D}_Q$-stabilization theory to ensure that the eigenvalues of the closed-loop system lie in a specified domain within the unit disk by constructing a sufficiency condition in the form of a data-driven linear matrix inequality (LMI).

Notations: $\mathbb{R}^{\ell}$ and $\mathbb{R}^{\ell\times\jmath}$ represent the ℓ-dimensional column vector and the $\ell\times\jmath$-dimensional real matrix, respectively. I and $\mathbf{0}_{\ell\times\jmath}$ represent the unit matrix of the appropriate dimension and the zero matrix of $\ell\times\jmath$ dimensions. $\Upsilon>0$ ($\Upsilon\geq 0$, $\Upsilon<0$, $\Upsilon\leq 0$) represents Υ being a positive-definite (positive-semidefinite, negative-definite, negative-semidefinite) matrix. $\Upsilon^{\top}$ (Υ^{-1}) represents the transpose (inverse) of matrix Υ. $\ker(\Upsilon)$ represents the kernel of the matrix Υ.

2. System description and problem formulation

In this section, the mathematical models of each DGU are presented, and then the distributed voltage regulation problem is introduced.

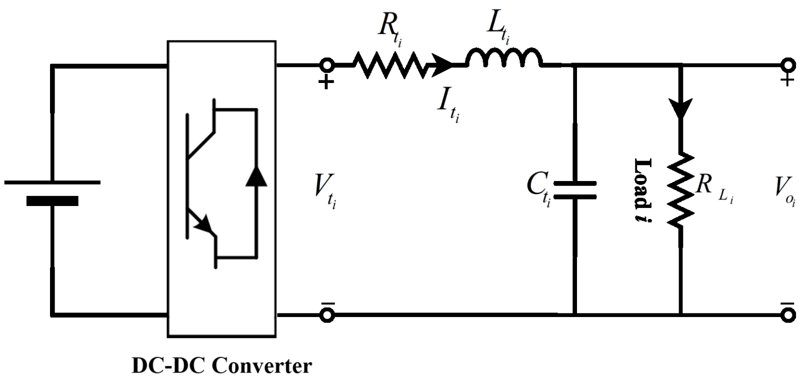

Figure 1. DGU i in a DC microgrid.

Consider that a DC microgrid consists of N DGUs, and the DGU i is shown as Figure 1, which consists of a DC voltage source, a resistor-inductor (RL) filter, a capacitor, and a load. V_{t_i}, I_{t_i}, and V_{o_i} are the converter terminal voltage, the series RL filter current, and the load voltage of DGU i, respectively. The dynamics of DGU i are described as follows:

$$\text{DGU } i: \begin{cases} \frac{\mathrm{d}V_{o_i}}{\mathrm{d}t} &= \frac{1}{C_{t_i}}\left(I_{t_i}-\frac{V_{o_i}}{R_{L_i}}\right), \\ \frac{\mathrm{d}I_{t_i}}{\mathrm{d}t} &= \frac{1}{L_{t_i}}\left(V_{t_i}-V_{o_i}-R_{t_i}I_{t_i}\right), \end{cases} \quad i=1,2,\ldots,N, \tag{2.1}$$

where the specific values of the inductor L_{t_i}, capacitor C_{t_i}, as well as resistors R_{t_i} and R_{L_i} are unknown.

Define $x_i \triangleq \begin{bmatrix} V_{o_i} & I_{t_i} \end{bmatrix}^{\top} \in \mathbb{R}^2$, $u_i \triangleq V_{t_i} \in \mathbb{R}^1$, and $y_i \triangleq V_{o_i} \in \mathbb{R}^1$ as the state, control input, and output of DGU i, respectively, and then the dynamics of DGU i (2.1) can be modeled as the following continuous-time state-space equation:

$$\begin{cases} \dot{x}_i(t) &= A_i^c x_i(t) + B_i^c u_i(t), \\ y_i(t) &= C_i x_i(t), \end{cases} \quad i = 1, 2, \ldots, N, \tag{2.2}$$

where $A_i^c = \begin{bmatrix} -\frac{1}{C_{t_i} R_{L_i}} & \frac{1}{C_{t_i}} \\ -\frac{1}{L_{t_i}} & -\frac{R_{t_i}}{L_{t_i}} \end{bmatrix}$, $B_i^c = \begin{bmatrix} 0 \\ \frac{1}{L_{t_i}} \end{bmatrix}$, and $C_i = \begin{bmatrix} 1 \\ 0 \end{bmatrix}^{\mathrm{T}}$. Due to the unknown values of inductor, capacitor, and resistors in the DGU i, the system matrices A_i and B_i are also unknown.

Because the signal transmission among DGUs is carried out in discrete sequences, we discretize the continuous-time state-space equation (2.2) with a sampling period of T_d as the following discrete-time state-space equation:

$$\begin{cases} x_i(k+1) &= A_i x_i(k) + B_i u_i(k), \\ y_i(k) &= C_i x_i(k), \end{cases} \quad i = 1, 2, \ldots, N, \tag{2.3}$$

where $A_i = e^{A_i^c T_d}$, $B_i = \int_0^{T_d} e^{A_i^c t} B_i^c \mathrm{d}t$, and k denotes the kth sampling moment, which can be directly calculated using the `c2d` command in MATLAB.

The desired reference signal is generated by

$$\begin{cases} x_r(k+1) &= D x_r(k), \\ y_r(k) &= E x_r(k), \end{cases} \tag{2.4}$$

where $x_r(k) \in \mathbb{R}^r$ and $y_r(k) \in \mathbb{R}^1$ stand for the state and output of the reference signal. The dynamic system (2.4) can generate various types of reference signal, such as constant signal, sine/cosine signal, and their combinations, etc. The control protocols designed in [21, 22] can only ensure that the DC microgrids track constant signal. In this paper, we will design a distributed control protocol to enable the DC microgrids to track various types of reference signal.

Consider the communication topology among the N DGUs given in (2.3) described by a directed graph $\mathscr{G} = \{\mathscr{V}, \mathscr{E}, \mathscr{A}\}$. $\mathscr{V} = \{1, \ldots, N\}$ denotes the DGU set. $\mathscr{E} \subset \mathscr{V} \times \mathscr{V}$ denotes the set of edges. $\mathscr{A} = [a_{ij}] \in \mathbb{R}^{N \times N}$ denotes the adjacency matrix where the weight $a_{ij} > 0$ if DGU i can receive information from DGU j and $a_{ij} = 0$ otherwise. Moreover, the pinning gain of DGU i is h_i with $h_i > 0$ if the reference signal is pinned to DGU i and $h_i = 0$ otherwise.

As can be seen from [23–25], several standard assumptions for the feasibility of the distributed control problem need to be imposed on the systems (2.3) and (2.4).

Assumption 1. *For $i = 1, 2, \ldots, N$,* Rank$\begin{bmatrix} A_i - \lambda I & B_i \\ C_i & 0 \end{bmatrix} = 3$, *$\forall \lambda \in \sigma(D)$, where $\sigma(D)$ denotes the spectrum of D.*

Assumption 2. *For $i = 1, 2, \ldots, N$, the matrix pair (A_i, B_i) is controllable.*

Assumption 3. *The graph $\mathscr{G}$ has a directed spanning tree with the reference signal as the root node.*

Remark 1. *Assumption 1 is to prevent the case of zero-pole cancellation. If the system has irreversible transmission zeros, it may cause unstable behavior. The rank condition in Assumption 1 eliminates this case. Assumption 2 is the fundamental engineering prerequisite for controlling the DC microgrid.*

Each DGU must be controllable in order to achieve cooperative voltage regulation of the entire DC microgrid. Assumption 3 states that the information of the reference signal is guaranteed to be globally accessible. If the reference signal cannot reach certain DGUs through the communication network, these DGUs will have no idea about which reference signal to track.

Problem 1. *The cooperative voltage regulation problem is to design a distributed control protocol $u_i(k)$ such that the output y_i of each DGU described by (2.3) can asymptotically track the desired reference signal y_r generated by (2.4), i.e., $\lim_{k\to\infty}(y_i(k) - y_r(k)) = 0$, $i = 1, 2, \ldots, N$.*

3. Main results

In this section, we first present the specific structure of the distributed control protocol based on the internal model principle. Then, the model- and data-based design methods for the gain matrices of the distributed control protocol are provided.

3.1. Internal model-based distributed control protocol

To address Problem 1, we design the following distributed control protocol:

$$\eta_i(k+1) = \mathcal{Z}_1\eta_i(k) + \mathcal{Z}_2\left[\sum_{j=1}^{N} a_{ij}\left(y_i(k) - y_j(k)\right) + h_i(y_i(k) - y_r(k))\right], \tag{3.1}$$

$$u_i(k) = \mathcal{K}_i^1 x_i(k) + \mathcal{K}_i^2\eta_i(k), \tag{3.2}$$

where the matrix pair $(\mathcal{Z}_1, \mathcal{Z}_2)$ constitutes a 1-copy internal model of the matrix D, and $\mathcal{K}_i^1$ and $\mathcal{K}_i^2$ are the gain matrices that need to be designed. Moreover, consider that the communication weights of the graph are normalized: $\sum_{j=1}^{N} a_{ij} + h_i = 1$ for $i = 1, 2, \ldots, N$. From the control protocol (3.1), it can be seen that DGU i only utilizes the output of its neighboring DGU. This indicates that all DGUs only transmit the output voltage V_{o_i} during interacting, which is different from [13, 14, 17, 18], where the state of the neighboring DGUs, namely the voltage V_{o_i} and current I_{t_i}, needs to be transmitted. This makes the designed control protocol in our paper more suitable for use in actual DC microgrids.

Based on the system matrix D in the reference signal (2.4), $\mathcal{Z}_1$ and $\mathcal{Z}_2$ can be selected in the following form:

$$\mathcal{Z}_1 = \begin{bmatrix} 0 & 1 & \cdots & 0 \\ 0 & 0 & \cdots & 0 \\ \vdots & \vdots & \ddots & \vdots \\ 0 & 0 & \cdots & 1 \\ -p_r & -p_{r-1} & \cdots & -p_1 \end{bmatrix}, \ \mathcal{Z}_2 = \begin{bmatrix} 0 \\ 0 \\ \vdots \\ 0 \\ 1 \end{bmatrix}, \tag{3.3}$$

where p_ℓ, $\ell = 1, 2, \ldots, r$ is the coefficients of the minimal polynomial of the system matrix D: $p_\ell(\lambda) = \lambda^r + p_1\lambda^{r-1} + \cdots + p_{r-1}\lambda + p_r$.

Remark 2. *In decentralized control, each DGU operates independently based solely on its own measurements with no communication between DGUs, but each DGU needs to know the information of the reference signal. In distributed control, each DGU needs to obtain the information of its neighbors over communication network, but only one or few of the DGUs need to know the* *information of the reference signal. In [26], the novel prescribed-time decentralized and distributed output-feedback controllers were proposed, which has established a unified framework for decentralized and distributed control. Therefore, the integrated decentralized-distributed control frameworks will be the focus of our future research.*

Next, the model-based design method for the gain matrices $\mathcal{K}_i^1$ and $\mathcal{K}_i^2$ is presented. Furthermore, it demonstrates that Problem 1 can be transformed from a cooperative voltage regulation problem into a local stabilization problem.

3.2. Model-based design for gain matrices

By employing the distributed control protocol (3.1) and (3.2), we demonstrate that Problem 1 has been resolved.

Theorem 1. *Suppose that Assumptions 1–3 hold. The cooperative voltage regulation problem described as Problem 1 is addressed if the distributed control protocol (3.1) and (3.2) is used and the augmented gain matrix* $\mathcal{K}_i = \begin{bmatrix} \mathcal{K}_i^1 & \mathcal{K}_i^2 \end{bmatrix}$ *is designed as* $\mathcal{K}_i = \mathcal{K}_i^P \mathcal{P}_i^{-1}$*, where* $\mathcal{K}_i^P \in \mathbb{R}^{1\times(2+r)}$ *and* $\mathcal{P}_i^\top = \mathcal{P}_i \in \mathbb{R}^{(2+r)\times(2+r)} > 0$ *is subject to the following LMI:*

$$\begin{bmatrix} \mathcal{P}_i & \mathcal{A}_i\mathcal{P}_i + \mathcal{B}_i\mathcal{K}_i^P \\ \mathcal{P}_i\mathcal{A}_i^\top + \left(\mathcal{K}_i^P\right)^\top \mathcal{B}_i^\top & \mathcal{P}_i \end{bmatrix} > 0,\ i = 1, 2, \ldots, N, \tag{3.4}$$

with $\mathcal{A}_i = \begin{bmatrix} A_i & \mathbf{0}_{2\times r} \\ \mathcal{Z}_2 C_i & \mathcal{Z}_1 \end{bmatrix}$ *and* $\mathcal{B}_i = \begin{bmatrix} B_i \\ \mathbf{0}_{r\times 1} \end{bmatrix}$.

Proof. By applying the Schur complement operation to LMI (3.4) and based on $\mathcal{K}_i^P = \mathcal{K}_i\mathcal{P}_i$, one has

$$\mathcal{P}_i - (\mathcal{A}_i + \mathcal{B}_i\mathcal{K}_i)\mathcal{P}_i(\mathcal{A}_i + \mathcal{B}_i\mathcal{K}_i)^\top > 0,\ i = 1, 2, \ldots, N. \tag{3.5}$$

This means that $\mathcal{A}_i + \mathcal{B}_i\mathcal{K}_i$, $i = 1, 2, \ldots, N$ is a Schur stable matrix. Then, it can be obtained from [23] that there exists a unique matrix triple $(\Pi_i, \Omega_i, \Lambda_i)$ to the following linear matrix equations:

$$\Pi_i D = \left(A_i + B_i\mathcal{K}_i^1\right)\Pi_i + B_i\mathcal{K}_i^2\Lambda_i, \tag{3.6}$$

$$\Lambda_i D = \mathcal{Z}_1\Lambda_i + \mathcal{Z}_2\left(C_i\Pi_i - E\right), \tag{3.7}$$

$$C_i\Pi_i = E. \tag{3.8}$$

Define $\delta_i(k) \triangleq x_i(k) - \Pi_i x_r(k)$ and $\varepsilon_i(k) \triangleq \eta_i(k) - \Lambda_i x_r(k)$. By combining the DGU system (2.3), reference signal (2.4), control protocol (3.1) and (3.2), and linear matrix equations (3.6) and (3.7), we have

$$\begin{aligned} \delta_i(k+1) &= x_i(k+1) - \Pi_i x_r(k+1) \\ &= A_i x_i(k) + B_i u_i(k) - \Pi_i D x_r(k) \\ &= A_i x_i(k) + B_i\left(\mathcal{K}_i^1 x_i(k) + \mathcal{K}_i^2\eta_i(k)\right) - \Pi_i D x_r(k) \\ &= \left(A_i + B_i\mathcal{K}_i^1\right)x_i(k) + B_i\mathcal{K}_i^2\eta_i(k) - \Pi_i D x_r(k) \\ &= \left(A_i + B_i\mathcal{K}_i^1\right)x_i(k) + B_i\mathcal{K}_i^2\eta_i(k) - \left(\left(A_i + B_i\mathcal{K}_i^1\right)\Pi_i + B_i\mathcal{K}_i^2\Lambda_i\right)x_r(k) \end{aligned}$$

$$= \left(A_i + B_i\mathcal{K}_i^1\right)\delta_i(k) + B_i\mathcal{K}_i^2\varepsilon_i(k) \tag{3.9}$$

and

$$\begin{aligned}
\varepsilon_i(k+1) &= \eta_i(k+1) - \Lambda_i x_r(k+1) \\
&= \mathcal{Z}_1\eta_i(k) + \mathcal{Z}_2\left[\sum_{j=1}^{N} a_{ij}\left(y_i(k) - y_j(k)\right) + h_i\left(y_i(k) - y_r(k)\right)\right] - \Lambda_i D x_r(k) \\
&= \mathcal{Z}_1\eta_i(k) + \mathcal{Z}_2 C_i x_i(k) - \mathcal{Z}_2\sum_{j=1}^{N} a_{ij} y_j(k) - h_i\mathcal{Z}_2 E x_r(k) - \Lambda_i D x_r(k) \\
&= \mathcal{Z}_1\eta_i(k) + \mathcal{Z}_2 C_i x_i(k) - \mathcal{Z}_2\sum_{j=1}^{N} a_{ij} y_j(k) - h_i\mathcal{Z}_2 E x_r(k) \\
&\quad - \left(\mathcal{Z}_1\Lambda_i + \mathcal{Z}_2\left(C_i\Pi_i - E\right)\right) x_r(k) \\
&= \mathcal{Z}_1\varepsilon_i(k) + \mathcal{Z}_2 C_i\delta_i(k) - \mathcal{Z}_2\sum_{j=1}^{N} a_{ij} C_j x_j(k) - h_i\mathcal{Z}_2 E x_r(k) + \mathcal{Z}_2 E x_r(k) \\
&= \mathcal{Z}_1\varepsilon_i(k) + \mathcal{Z}_2 C_i\delta_i(k) - \mathcal{Z}_2\sum_{j=1}^{N} a_{ij} C_j\delta_j(k),
\end{aligned} \tag{3.10}$$

where the third and sixth = hold due to $\sum_{j=1}^{N} a_{ij} + h_i = 1$.

Let $\xi_i(k) \triangleq \begin{bmatrix} \delta_i(k) \\ \varepsilon_i(k) \end{bmatrix}$, and the augmented system can be obtained as

$$\xi_i(k+1) = \left(\mathcal{A}_i + \mathcal{B}_i\mathcal{K}_i\right)\xi_i(k) - \sum_{j=1}^{N} a_{ij}\begin{bmatrix} \mathbf{0}_{2\times(2+r)} \\ \mathcal{Z}_2 C_j \end{bmatrix}\xi_j(k), \tag{3.11}$$

$$e_i(k) = \mathcal{C}_i\xi_i(k), \tag{3.12}$$

where $\mathcal{A}_i$ and $\mathcal{B}_i$ are given in (3.4), $\mathcal{K}_i = \begin{bmatrix} \mathcal{K}_i^1 & \mathcal{K}_i^2 \end{bmatrix}$, and $\mathcal{C}_i = \begin{bmatrix} C_i & \mathbf{0}_{1\times r} \end{bmatrix}$. Based on (3.8), one has $e_i(k) = \mathcal{C}_i\xi_i(k) = C_i\delta_i(k) = C_i\left(x_i(k) - \Pi_i x_r(k)\right) = y_i(k) - y_r(k)$, and thus $e_i(k)$ can be regarded as the tracking error.

Under Assumption 3, the label of all the DGUs can be rearranged such that $i > j$ if DGU i can receive information from DGU j. Then, the overall forms of (3.11) and (3.12) can be written as

$$\xi(k+1) = \left(\mathcal{A} + \mathcal{B}\mathcal{K}\right)\xi(k), \tag{3.13}$$

$$e(k) = \mathcal{C}\xi(k), \tag{3.14}$$

with

$$\begin{aligned}
\xi(k) &= \begin{bmatrix} \xi_1^\top(k) & \xi_2^\top(k) & \cdots & \xi_N^\top(k) \end{bmatrix}^\top, \\
e(k) &= \begin{bmatrix} e_1^\top(k) & e_2^\top(k) & \cdots & e_N^\top(k) \end{bmatrix}^\top, \\
\mathcal{A} &= \text{blockdiag}\left(\mathcal{A}_1, \mathcal{A}_2, \cdots, \mathcal{A}_N\right),
\end{aligned}$$

$$\mathcal{B} = \text{blockdiag}\left(\mathcal{B}_1, \mathcal{B}_2, \cdots, \mathcal{B}_N\right),$$
$$C = \text{blockdiag}\left(C_1, C_2, \cdots, C_N\right),$$
$$\mathcal{K} = \text{blockdiag}\left(\mathcal{K}_1, \mathcal{K}_2, \cdots, \mathcal{K}_N\right).$$

If LMI (3.4) holds, then $\mathcal{A}_i + \mathcal{B}_i\mathcal{K}_i$, $i = 1, 2, \ldots, N$ is a Schur stable matrix, namely, $\mathcal{A} + \mathcal{B}\mathcal{K}$ is a Schur stable matrix. This means that $\xi(k)$ is asymptotically stable, i.e., $\lim_{k\to\infty} \xi_i(k) = 0$, $i = 1, 2, \ldots, N$, then one has $\lim_{k\to\infty} e_i(k) = \lim_{k\to\infty} (y_i(k) - y_r(k)) = 0$. Therefore, the cooperative voltage regulation problem described as Problem 1 is addressed. The proof is concluded.

Remark 3. *From Theorem 1, it can be seen that if a control input $\hat{u}_i(k) = \mathcal{K}_i\xi_i(k)$ can stabilize $\xi_i(k+1) = \mathcal{A}_i\xi_i(k) + \mathcal{B}_i\hat{u}_i(k)$ (i.e., $\mathcal{A}_i + \mathcal{B}_i\mathcal{K}_i$, $i = 1, 2, \ldots, N$ is a Schur stable matrix), then Problem 1 is solved. This means that the original distributed tracking control problem can be transformed into a local stabilization problem, which can simplify the difficulty of solving the gain matrices. Therefore, we will focus on the local stabilization problem in the subsequent data-driven design approach.*

3.3. Data-driven robust design for gain matrices

Before presenting the data-driven design method, we introduce a series of lemmas that will be needed.

Lemma 1. *[27] The cooperative voltage regulation problem is addressed with $\mathcal{D}_Q$-stabilizable performance guarantee if and only if there exists a matrix $\hat{\mathcal{P}}_i^\top = \hat{\mathcal{P}}_i \in \mathbb{R}^{(2+r)\times(2+r)} > 0$ such that*

$$\begin{aligned}-Q_i^{11} \otimes \hat{\mathcal{P}}_i - Q_i^{12} \otimes \left(\hat{\mathcal{P}}_i (\mathcal{A}_i + \mathcal{B}_i\mathcal{K}_i)^\top\right) - \left(Q_i^{12}\right)^\top \otimes \left((\mathcal{A}_i + \mathcal{B}_i\mathcal{K}_i)\hat{\mathcal{P}}_i\right) \\ -Q_i^{22} \otimes \left((\mathcal{A}_i + \mathcal{B}_i\mathcal{K}_i)\hat{\mathcal{P}}_i (\mathcal{A}_i + \mathcal{B}_i\mathcal{K}_i)^\top\right) > 0,\ i = 1, 2, \ldots, N,\end{aligned} \tag{3.15}$$

where $\left(Q_i^{11}\right)^\top = Q_i^{11} \in \mathbb{R}^{n_i\times n_i}$, $\left(Q_i^{22}\right)^\top = Q_i^{22} \in \mathbb{R}^{n_i\times n_i} \geq 0$, and they form $Q_i = \begin{bmatrix} Q_i^{11} & Q_i^{12} \\ \left(Q_i^{12}\right)^\top & Q_i^{22} \end{bmatrix} \in \mathbb{R}^{2n_i\times 2n_i}$.

Proof. By selecting Q_i^{11}, Q_i^{12}, and Q_i^{22} [27], the augmented gain matrix $\mathcal{K}_i$ can be designed from (3.15) such that the eigenvalues of $\mathcal{A}_i + \mathcal{B}_i\mathcal{K}_i$, $i = 1, 2, \ldots, N$ lie in a specified domain within the unit disk, i.e., $\mathcal{A}_i + \mathcal{B}_i\mathcal{K}_i$ is a Schur stable matrix. Then, it can be known from Theorem 1 that the cooperative voltage regulation problem is addressed.

Lemma 2. *[28] Given two matrices as $\mathcal{S}_i = \begin{bmatrix} \mathcal{S}_i^{11} & \mathcal{S}_i^{12} \\ \left(\mathcal{S}_i^{12}\right)^\top & \mathcal{S}_i^{22} \end{bmatrix}$ and $\mathcal{V}_i = \begin{bmatrix} \mathcal{V}_i^{11} & \mathcal{V}_i^{12} \\ \left(\mathcal{V}_i^{12}\right)^\top & \mathcal{V}_i^{22} \end{bmatrix}$ with $\mathcal{S}_i^{22} \leq 0$, $\mathcal{V}_i^{22} \leq 0$ and $\ker\left(\mathcal{V}_i^{22}\right) \subseteq \ker\left(\mathcal{V}_i^{12}\right)$. Then, $\begin{bmatrix} I \\ F_i \end{bmatrix}^\top \mathcal{S}_i \begin{bmatrix} I \\ F_i \end{bmatrix} > 0$ with $\begin{bmatrix} I \\ F_i \end{bmatrix}^\top \mathcal{V}_i \begin{bmatrix} I \\ F_i \end{bmatrix} \geq 0$ if and only if there exist scalars $\mu_i \geq 0$ and $\upsilon_i > 0$ such that $\mathcal{S}_i - \mu_i\mathcal{V}_i \geq \begin{bmatrix} \upsilon_i I & 0 \\ 0 & 0 \end{bmatrix}$.*

3.3.1. Data collection

It can be seen from (3.9) and (3.10) that the error variables $\delta_i(k)$ and $\varepsilon_i(k)$ are coupled with the solutions of (3.6)–(3.8), and the determination of matrix triple $(\Pi_i, \Omega_i, \Lambda_i)$ requires system parameter information. To avoid exploiting the system parameter information of A_i and B_i, we adopted the following auxiliary system during the data collection stage:

$$\hat{\eta}_i(k+1) = \mathcal{Z}_1\hat{\eta}_i(k) + \mathcal{Z}_2 y_i(k), \tag{3.16}$$

where $\mathcal{Z}_1$ and $\mathcal{Z}_2$ can be chosen as (3.3).

Applying a persistently exciting input $u_i^d(k)$ to each DGU (2.3) and letting $\hat{\xi}_i(k) \triangleq \begin{bmatrix} x_i^\top(k) & \hat{\eta}_i^\top(k) \end{bmatrix}^\top$, we have

$$\hat{\xi}_i(k+1) = \mathcal{A}_i\hat{\xi}_i(k) + \mathcal{B}_i u_i^d(k), \tag{3.17}$$

where $\mathcal{A}_i$ and $\mathcal{B}_i$ are given in (3.4). It is obvious that the system (3.17) and the error system (3.13) have the same structure. Therefore, we can use the offline data of the system (3.17) to design the augmented gain matrix $\mathcal{K}_i$. Furthermore, it is considered that the system (3.17) is affected by unknown noise during data collection. The state and input data of the system (3.17) are obtained from the following noisy system:

$$\hat{\xi}_i(k+1) = \mathcal{A}_i\hat{\xi}_i(k) + \mathcal{B}_i u_i^d(k) + \omega_i(k), \tag{3.18}$$

where $\omega_i(k) \in \mathbb{R}^{(2+r)}$ is the unknown noise. Performing $\mathcal{T}_i$, $i = 1, 2, \ldots, N$ experiments on the system (3.18) results in the following state and input data:

$$\begin{aligned} \Xi_i &= \left[\begin{array}{cccc} x_i(0) & x_i(1) & \cdots & x_i(\mathcal{T}_i) \\ \hline \hat{\eta}_i(0) & \hat{\eta}_i(1) & \cdots & \hat{\eta}_i(\mathcal{T}_i) \end{array}\right], \\ \mathcal{U}_i^- &= \begin{bmatrix} u_i^d(0) & u_i^d(1) & \cdots & u_i^d(\mathcal{T}_i - 1) \end{bmatrix}. \end{aligned} \tag{3.19}$$

Based on the noisy system (3.18) and dataset (3.19), one has

$$\Xi_i^+ = \mathcal{A}_i\Xi_i^- + \mathcal{B}_i\mathcal{U}_i^- + \mathcal{W}_i^-, \tag{3.20}$$

where

$$\begin{aligned} \Xi_i^+ &= \left[\begin{array}{cccc} x_i(1) & x_i(2) & \cdots & x_i(\mathcal{T}_i) \\ \hline \hat{\eta}_i(1) & \hat{\eta}_i(2) & \cdots & \hat{\eta}_i(\mathcal{T}_i) \end{array}\right], \\ \Xi_i^- &= \left[\begin{array}{cccc} x_i(0) & x_i(1) & \cdots & x_i(\mathcal{T}_i - 1) \\ \hline \hat{\eta}_i(0) & \hat{\eta}_i(1) & \cdots & \hat{\eta}_i(\mathcal{T}_i - 1) \end{array}\right], \\ \mathcal{W}_i^- &= \begin{bmatrix} \omega_i(0) & \omega_i(1) & \cdots & \omega_i(\mathcal{T}_i - 1) \end{bmatrix}. \end{aligned}$$

Note that $\mathcal{W}_i^-$ is unknown. Moreover, we suppose that $\mathcal{W}_i^- \in \hat{\mathcal{W}}_i$ and the set $\hat{\mathcal{W}}_i$ is defined as

$$\hat{\mathcal{W}}_i \triangleq \left\{ \mathcal{W}_i \middle| \begin{bmatrix} I \\ \mathcal{W}_i^\top \end{bmatrix}^\top \begin{bmatrix} O_i^{11} & O_i^{12} \\ \left(O_i^{12}\right)^\top & O_i^{22} \end{bmatrix} \begin{bmatrix} I \\ \mathcal{W}_i^\top \end{bmatrix} \geq 0 \right\}, \tag{3.21}$$

where $\left(O_i^{11}\right)^\top = O_i^{11} \in \mathbb{R}^{(2+r)\times(2+r)}$, $\left(O_i^{22}\right)^\top = O_i^{22} \in \mathbb{R}^{\mathcal{T}_i\times\mathcal{T}_i} < 0$, and $O_i^{12} \in \mathbb{R}^{(2+r)\times\mathcal{T}_i}$ are the known matrices.

Remark 4. *In this paper, we focus on additive measurement noise. However, the multiplicative noise is common in sensor measurement [29]. If the current and/or voltage data are affected by multiplicative noise, it will affect the authenticity of the collected data. When the multiplicative noise is large, the proposed methods will fail. Therefore, how to quantify the impact of multiplicative noise on the robustness of microgrids will be one of our next works.*

Next, we utilize Lemmas 1 and 2 along with the collected data $\left(\Xi_i^+, \Xi_i^-, \mathcal{U}_i^-\right)$ to design a data-driven robust method for solving the augmented gain matrix $\mathcal{K}_i$ such that $\mathcal{A}_i + \mathcal{B}_i\mathcal{K}_i$ is a Schur stable matrix for $i = 1, 2, \ldots, N$.

3.3.2. Data-driven robust design

Define Ω_i as all possible systems that can explain the dataset Ξ_i^+, Ξ_i^-, and $\mathcal{U}_i^-$, which satisfies set $\hat{\mathcal{W}}_i$, and it is defined as

$$\Omega_i \triangleq \left\{\left(\hat{\mathcal{A}}_i, \hat{\mathcal{B}}_i\right) \middle| \Xi_i^+ - \hat{\mathcal{A}}_i\Xi_i^- - \hat{\mathcal{B}}_i\mathcal{U}_i^- \in \hat{\mathcal{W}}_i\right\}. \tag{3.22}$$

It should be noted that $(\mathcal{A}_i, \mathcal{B}_i) \in \Omega_i$ and Ω_i is a non-single-element set.

For $(\mathcal{A}_i, \mathcal{B}_i) \in \Omega_i$ and $\mathcal{W}_i^- \in \hat{\mathcal{W}}_i$, $\Xi_i^+ - \hat{\mathcal{A}}_i\Xi_i^- - \hat{\mathcal{B}}_i\mathcal{U}_i^- = \mathcal{W}_i^- \in \hat{\mathcal{W}}_i$. Based on (3.21), we have

$$\begin{bmatrix} I \\ \begin{bmatrix} \hat{\mathcal{A}}_i & \hat{\mathcal{B}}_i \end{bmatrix}^\top \end{bmatrix}^\top \begin{bmatrix} I & \Xi_i^+ \\ \mathbf{0}_{(2+r)\times(2+r)} & -\Xi_i^- \\ \mathbf{0}_{(2+r)\times(2+r)} & -\mathcal{U}_i^- \end{bmatrix} \begin{bmatrix} O_i^{11} & O_i^{12} \\ \left(O_i^{12}\right)^\top & O_i^{22} \end{bmatrix} \begin{bmatrix} I & \Xi_i^+ \\ \mathbf{0}_{(2+r)\times(2+r)} & -\Xi_i^- \\ \mathbf{0}_{(2+r)\times(2+r)} & -\mathcal{U}_i^- \end{bmatrix}^\top \begin{bmatrix} I \\ \begin{bmatrix} \hat{\mathcal{A}}_i & \hat{\mathcal{B}}_i \end{bmatrix}^\top \end{bmatrix} \geq 0. \tag{3.23}$$

Back to Lemma 1 and due to $(\mathcal{A}_i, \mathcal{B}_i) \in \Omega_i$, the eigenvalues of $\mathcal{A}_i + \mathcal{B}_i\mathcal{K}_i$, $i = 1, 2, \ldots, N$ can lie in a specified domain within the unit disk if the inequality (3.15) holds for all $\left(\hat{\mathcal{A}}_i, \hat{\mathcal{B}}_i\right) \in \Omega_i$. Then, the inequality (3.15) is reconstructed as

$$\begin{bmatrix} I \\ I \otimes \begin{bmatrix} \hat{\mathcal{A}}_i & \hat{\mathcal{B}}_i \end{bmatrix}^\top \end{bmatrix}^\top \mathcal{S}_i \begin{bmatrix} I \\ I \otimes \begin{bmatrix} \hat{\mathcal{A}}_i & \hat{\mathcal{B}}_i \end{bmatrix}^\top \end{bmatrix} > 0, \tag{3.24}$$

where

$$\mathcal{S}_i = \left[\begin{array}{c|cc} -Q_i^{11} \otimes \hat{\mathcal{P}}_i & -Q_i^{12} \otimes \hat{\mathcal{P}}_i & -Q_i^{12} \otimes \left(\hat{\mathcal{P}}_i\mathcal{K}_i^\top\right) \\ \hline -\left(Q_i^{12}\right)^\top \otimes \hat{\mathcal{P}}_i & -Q_i^{22} \otimes \hat{\mathcal{P}}_i & -Q_i^{22} \otimes \left(\hat{\mathcal{P}}_i\mathcal{K}_i^\top\right) \\ -\left(Q_i^{12}\right)^\top \otimes \left(\mathcal{K}_i\hat{\mathcal{P}}_i\right) & -Q_i^{22} \otimes \left(\mathcal{K}_i\hat{\mathcal{P}}_i\right) & -Q_i^{22} \otimes \left(\mathcal{K}_i\hat{\mathcal{P}}_i\mathcal{K}_i^\top\right) \end{array}\right].$$

Lemma 1 holds if and only if the inequality (3.24) holds for all $\left(\hat{\mathcal{A}}_i, \hat{\mathcal{B}}_i\right) \in \Omega_i$, and thus we next construct conditions to ensure that the inequality (3.24) holds. To this end, we reconstruct the inequality (3.23) as

$$\begin{bmatrix} I \\ I \otimes \begin{bmatrix} \hat{\mathcal{A}}_i & \hat{\mathcal{B}}_i \end{bmatrix}^\top \end{bmatrix}^\top \mathcal{V}_i \begin{bmatrix} I \\ I \otimes \begin{bmatrix} \hat{\mathcal{A}}_i & \hat{\mathcal{B}}_i \end{bmatrix}^\top \end{bmatrix} > 0, \tag{3.25}$$

where

$$\mathcal{V}_i = \left[\begin{array}{cc} I & I \otimes \Xi_i^+ \\ \hline \mathbf{0}_{n_i(2+r)\times n_i(2+r)} & -I \otimes \Xi_i^- \\ \mathbf{0}_{n_i(2+r)\times n_i(2+r)} & -I \otimes \mathcal{U}_i^- \end{array}\right] \begin{bmatrix} I \otimes O_i^{11} & I \otimes O_i^{12} \\ I \otimes \left(O_i^{12}\right)^\top & I \otimes O_i^{22} \end{bmatrix} \left[\begin{array}{cc} I & I \otimes \Xi_i^+ \\ \hline \mathbf{0}_{n_i(2+r)\times n_i(2+r)} & -I \otimes \Xi_i^- \\ \mathbf{0}_{n_i(2+r)\times n_i(2+r)} & -I \otimes \mathcal{U}_i^- \end{array}\right]^\top.$$

Let $F_i \triangleq I \otimes \begin{bmatrix} \hat{\mathcal{A}}_i & \hat{\mathcal{B}}_i \end{bmatrix}^\top$, and based on $\mathcal{S}_i$ and $\mathcal{V}_i$ defined in Lemma 2 and reconstructed in (3.24) and (3.25), we have

$$\begin{aligned} \mathcal{S}_i^{22} &= \begin{bmatrix} -Q_i^{22} \otimes \hat{\mathcal{P}}_i & -Q_i^{22} \otimes \left(\hat{\mathcal{P}}_i \mathcal{K}_i^\top\right) \\ -Q_i^{22} \otimes \left(\mathcal{K}_i \hat{\mathcal{P}}_i\right) & -Q_i^{22} \otimes \left(\mathcal{K}_i \hat{\mathcal{P}}_i \mathcal{K}_i^\top\right) \end{bmatrix} \\ &= -\begin{bmatrix} M \otimes I \\ M \otimes \mathcal{K}_i \end{bmatrix} \left(I \otimes \hat{\mathcal{P}}_i\right) \begin{bmatrix} M \otimes I \\ M \otimes \mathcal{K}_i \end{bmatrix}^\top, \end{aligned} \tag{3.26}$$

$$\mathcal{V}_i^{12} = \left(I \otimes O_i^{12} + I \otimes \Xi_i^+ O_i^{22}\right) \begin{bmatrix} I \otimes \Xi_i^- \\ I \otimes \mathcal{U}_i^- \end{bmatrix}^\top, \tag{3.27}$$

$$\mathcal{V}_i^{22} = \begin{bmatrix} I \otimes \Xi_i^- \\ I \otimes \mathcal{U}_i^- \end{bmatrix} \left(I \otimes O_i^{22}\right) \begin{bmatrix} I \otimes \Xi_i^- \\ I \otimes \mathcal{U}_i^- \end{bmatrix}^\top, \tag{3.28}$$

where $Q_i^{22} = MM^\top$.

Due to $\hat{\mathcal{P}}_i^\top = \hat{\mathcal{P}}_i \in \mathbb{R}^{(2+r)\times(2+r)} > 0$, it can be seen from (3.26) that $\mathcal{S}_i^{22} \leq 0$. Because of $\left(O_i^{22}\right)^\top = O_i^{22} \in \mathbb{R}^{\mathcal{T}_i \times \mathcal{T}_i} < 0$ in (3.21), it follows from (3.28) that $\mathcal{V}_i^{22} \leq 0$. It is obvious from (3.28) that $\ker\left(\mathcal{V}_i^{22}\right) = \ker\left(\begin{bmatrix} I \otimes \Xi_i^- \\ I \otimes \mathcal{U}_i^- \end{bmatrix}^\top\right)$, and thus $\ker\left(\mathcal{V}_i^{22}\right) \subseteq \ker\left(\mathcal{V}_i^{12}\right)$. Given the establishment of these conditions, all that is needed next is to ensure the validity of the following theorem, which will guarantee the validity of $\begin{bmatrix} I \\ F_i \end{bmatrix}^\top \mathcal{S}_i \begin{bmatrix} I \\ F_i \end{bmatrix} > 0$ with $\begin{bmatrix} I \\ F_i \end{bmatrix}^\top \mathcal{V}_i \begin{bmatrix} I \\ F_i \end{bmatrix} \geq 0$ with $F_i = I \otimes \begin{bmatrix} \hat{\mathcal{A}}_i & \hat{\mathcal{B}}_i \end{bmatrix}^\top$. Then, Lemma 1 holds for all $\left(\hat{\mathcal{A}}_i, \hat{\mathcal{B}}_i\right) \in \Omega_i$.

Theorem 2. *Suppose that Assumptions 1–3 hold. The cooperative voltage regulation problem is addressed with $\mathcal{D}_Q$-stabilizable performance guarantee that if there exists a matrix $\hat{\mathcal{K}}_i \in \mathbb{R}^{1\times(2+r)}$, $\hat{\mathcal{P}}_i^\top = \hat{\mathcal{P}}_i \in \mathbb{R}^{(2+r)\times(2+r)} > 0$, scalars $\mu_i \geq 0$ and $\upsilon_i > 0$ such that*

$$\hat{\mathcal{S}}_i - \mu_i \hat{\mathcal{V}}_i \geq 0, \ i = 1, 2, \ldots, N, \tag{3.29}$$

with

$$\hat{\mathcal{S}}_i = \begin{bmatrix} -Q_i^{11} \otimes \hat{\mathcal{P}}_i - \upsilon_i I & -Q_i^{12} \otimes \hat{\mathcal{P}}_i & -Q_i^{12} \otimes \hat{\mathcal{K}}_i^\top & \mathbf{0}_{n_i(2+r)\times n_i(2+r)} \\ -\left(Q_i^{12}\right)^\top \otimes \hat{\mathcal{P}}_i & -Q_i^{22} \otimes \hat{\mathcal{P}}_i & -Q_i^{22} \otimes \hat{\mathcal{K}}_i^\top & \mathbf{0}_{n_i(2+r)\times n_i(2+r)} \\ -\left(Q_i^{12}\right)^\top \otimes \hat{\mathcal{K}}_i & -Q_i^{22} \otimes \hat{\mathcal{K}}_i & \mathbf{0}_{n_i \times n_i} & M \otimes \hat{\mathcal{K}}_i \\ \mathbf{0}_{n_i(2+r)\times n_i(2+r)} & \mathbf{0}_{n_i(2+r)\times n_i(2+r)} & M^\top \otimes \hat{\mathcal{K}}_i^\top & I \otimes \hat{\mathcal{P}}_i \end{bmatrix},$$

$$\hat{\mathcal{V}}_i = \left[\begin{array}{cc} I & I \otimes \Xi_i^+ \\ \hline \mathbf{0}_{n_i(2+r)\times n_i(2+r)} & -I \otimes \Xi_i^- \\ \mathbf{0}_{n_i \times n_i(2+r)} & -I \otimes \mathcal{U}_i^- \\ \mathbf{0}_{n_i(2+r)\times n_i(2+r)} & \mathbf{0}_{n_i(2+r)\times n_i \mathcal{T}_i} \end{array}\right] \begin{bmatrix} I \otimes O_i^{11} & I \otimes O_i^{12} \\ I \otimes \left(O_i^{12}\right)^\top & I \otimes O_i^{22} \end{bmatrix} \left[\begin{array}{cc} I & I \otimes \Xi_i^+ \\ \hline \mathbf{0}_{n_i(2+r)\times n_i(2+r)} & -I \otimes \Xi_i^- \\ \mathbf{0}_{n_i(2+r)\times n_i(2+r)} & -I \otimes \mathcal{U}_i^- \\ \mathbf{0}_{n_i(2+r)\times n_i(2+r)} & \mathbf{0}_{n_i(2+r)\times n_i \mathcal{T}_i} \end{array}\right]^\top,$$

where M is given in (3.26). Then, the augmented gain matrix is designed as $\mathcal{K}_i = \hat{\mathcal{K}}_i \hat{\mathcal{P}}_i^{-1}$.

Proof. If LMI (3.29) holds, $\hat{\mathcal{K}}_i \in \mathbb{R}^{1\times(2+r)}$, $\hat{\mathcal{P}}_i^\top = \hat{\mathcal{P}}_i \in \mathbb{R}^{(2+r)\times(2+r)} > 0$, and scalars $\mu_i \geq 0$ and $\upsilon_i > 0$

exist. Let $\hat{\mathcal{K}}_i = \mathcal{K}_i\hat{\mathcal{P}}_i$, and applying the Schur complement operation to LMI (3.29), one has

$$\mathcal{S}_i - \mu_i\mathcal{V}_i \geq \begin{bmatrix} \upsilon_i I & \mathbf{0}_{n_i(2+r)\times n_i(2+r)} & \mathbf{0}_{n_i(2+r)\times n_i} \\ \mathbf{0}_{n_i(2+r)\times n_i(2+r)} & \mathbf{0}_{n_i(2+r)\times n_i(2+r)} & \mathbf{0}_{n_i(2+r)\times n_i} \\ \mathbf{0}_{n_i\times n_i(2+r)} & \mathbf{0}_{n_i\times n_i(2+r)} & \mathbf{0}_{n_i\times n_i} \end{bmatrix}, \; i = 1, 2, \ldots, N, \tag{3.30}$$

where $\mathcal{S}_i$ and $\mathcal{V}_i$ are given in (3.24) and (3.25). From Lemma 2, we have $\begin{bmatrix} I \\ F_i \end{bmatrix}^\top \mathcal{S}_i \begin{bmatrix} I \\ F_i \end{bmatrix} > 0$ with $\begin{bmatrix} I \\ F_i \end{bmatrix}^\top \mathcal{V}_i \begin{bmatrix} I \\ F_i \end{bmatrix} \geq 0$ with $F_i = I \otimes \begin{bmatrix} \hat{\mathcal{A}}_i & \hat{\mathcal{B}}_i \end{bmatrix}^\top$. Then, the inequality (3.15) holds. By Lemma 1, the cooperative voltage regulation problem is addressed with $\mathcal{D}_Q$-stabilizable performance guarantee.

For the stabilization purpose of the error system (3.13), it is required that the eigenvalues of $\mathcal{A}_i + \mathcal{B}_i\mathcal{K}_i$, $i = 1, 2, \ldots, N$ lie in a specified domain within the unit disk. Therefore, Q_i in (3.15) can be selected as

$$Q_i = \begin{bmatrix} -r_i^2 & 0 \\ 0 & 1 \end{bmatrix}, \tag{3.31}$$

which can ensure that the eigenvalues of $\mathcal{A}_i + \mathcal{B}_i\mathcal{K}_i$ lie within the circle centered at the origin with a radius of $r_i \in [0, 1)$, $i = 1, 2, \ldots, N$. The closer the eigenvalues of $\mathcal{A}_i + \mathcal{B}_i\mathcal{K}_i$ are to the origin, the faster the convergence speed of the error system (3.13) can be achieved. However, due to the presence of unknown noise, it results in the inability to configure the eigenvalues of $\mathcal{A}_i + \mathcal{B}_i\mathcal{K}_i$ close to the origin. This is reflected in the fact that the data-driven LMI (3.29) does not hold.

Corollary 1. *Suppose that Assumptions 1–3 hold, and let Q_i defined in (3.31). The cooperative voltage regulation problem is addressed with the eigenvalues of $\mathcal{A}_i + \mathcal{B}_i\mathcal{K}_i$ lying within the circle centered at the origin with a radius of $r_i \in [0, 1)$ if there exists a matrix $\hat{\mathcal{K}}_i \in \mathbb{R}^{1\times(2+r)}$, $\hat{\mathcal{P}}_i^\top = \hat{\mathcal{P}}_i \in \mathbb{R}^{(2+r)\times(2+r)} > 0$, scalars $\mu_i \geq 0$ and $\upsilon_i > 0$ such that*

$$\begin{bmatrix} r_i^2\hat{\mathcal{P}}_i - \upsilon_i I & \mathbf{0}_{(2+r)\times(2+r)} & \mathbf{0}_{(2+r)\times 1} & \mathbf{0}_{(2+r)\times(2+r)} \\ \mathbf{0}_{(2+r)\times(2+r)} & -\hat{\mathcal{P}}_i & -\hat{\mathcal{K}}_i^\top & \mathbf{0}_{(2+r)\times(2+r)} \\ \mathbf{0}_{1\times(2+r)} & -\hat{\mathcal{K}}_i & 0 & \hat{\mathcal{K}}_i \\ \mathbf{0}_{(2+r)\times(2+r)} & \mathbf{0}_{(2+r)\times(2+r)} & \hat{\mathcal{K}}_i^\top & \hat{\mathcal{P}}_i \end{bmatrix},$$

$$-\mu_i \left[\begin{array}{cc} I & \Xi_i^+ \\ \hline \mathbf{0}_{(2+r)\times(2+r)} & -\Xi_i^- \\ \mathbf{0}_{1\times(2+r)} & -\mathcal{U}_i^- \\ \mathbf{0}_{(2+r)\times(2+r)} & \mathbf{0}_{(2+r)\times\mathcal{T}_i} \end{array}\right] \begin{bmatrix} O_i^{11} & O_i^{12} \\ \left(O_i^{12}\right)^\top & O_i^{22} \end{bmatrix} \left[\begin{array}{cc} I & \Xi_i^+ \\ \hline \mathbf{0}_{(2+r)\times(2+r)} & -\Xi_i^- \\ \mathbf{0}_{1\times(2+r)} & -\mathcal{U}_i^- \\ \mathbf{0}_{(2+r)\times(2+r)} & \mathbf{0}_{(2+r)\times\mathcal{T}_i} \end{array}\right]^\top \geq 0, \; i = 1, 2, \ldots, N. \tag{3.32}$$

Then, the augmented gain matrix is designed as $\mathcal{K}_i = \hat{\mathcal{K}}_i\hat{\mathcal{P}}_i^{-1}$.

Proof. This corollary can be directly derived from Theorem 2 by setting $Q_i = \begin{bmatrix} -r_i^2 & 0 \\ 0 & 1 \end{bmatrix}$.

4. Simulation example

In this section, a numerical example is used to verify the effectiveness and robustness of the data-driven robust distributed control strategy. The DC microgrid is composed of six DGUs, and the communication topology among them is shown in Figure 2. It can be seen that only DGU 2 is able to obtain the output information of the reference signal, while the other DGUs can only obtain the output information of their neighboring DGUs. This indicates that a distributed communication pattern is employed among the DGUs. Moreover, the parameters of each DGU are provided in Table 1, which is borrowed from [22].

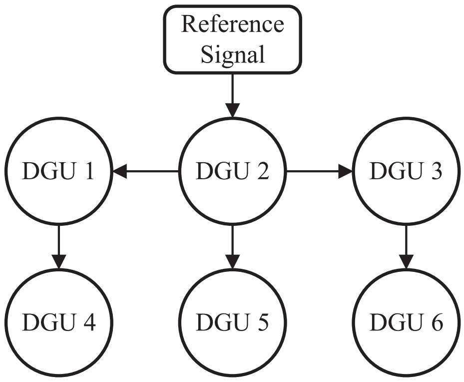

Figure 2. The communication topology among six DGUs.

Table 1. Electrical parameters of DGU i in Figure 1.

Parameters	DGU 1	DGU 2	DGU 3	DGU 4	DGU 5	DGU 6
L_{t_i} (mH)	1.8	2.0	2.2	3.0	1.2	2.5
R_{t_i} (Ω)	0.2	0.3	0.1	0.5	0.4	0.6
C_{t_i} (mF)	2.2	1.9	1.7	2.5	2.0	3.0
R_{L_i} (Ω)	10	6	20	2	4	8

In the simulation, the parameters of each DGU in Table 1 are supposed to be unknown, i.e., the system matrices A_i and B_i in (2.3) are unknown. Consequently, only the data generated by the system matrices A_i and B_i can be obtained. During the data collection stage, the state and input data are obtained from the system (3.18) affected by norm-bounded noise with $\|\omega_i(k)\| \leq \varpi_i = 0.01i$ for all $k \in [0, \mathcal{T}_i - 1]$ and $i = \{1, 2, \ldots, 6\}$. We can use the inequality (3.21) to describe the noise with $O_i^{11} = \mathcal{T}_i \varpi_i I$, $O_i^{12} = \mathbf{0}_{(2+r)\times\mathcal{T}_i}$, and $O_i^{22} = -I$, $i = \{1, 2, \ldots, 6\}$. The length of data collection is selected as $\mathcal{T}_i = 30$ for all $i = \{1, 2, \ldots, 6\}$.

It is verified that the proposed method enables each DGU to track constant signals. For this purpose, we select $D = 1$ and $E = 1$, and then one has $\mathcal{Z}_1 = 1$ and $\mathcal{Z}_2 = 1$ from (3.3). Then, we apply a persistently exciting input $u_i^d(k)$, $k \in [0, \mathcal{T}_i - 1]$ to each DGU (2.3) and randomly choose initial states $x_i(0)$ and $\hat{\eta}_i(0)$, and we can obtain dataset Ξ_i and $\mathcal{U}_i^-$ in (3.19). By substituting the dataset Ξ_i^+, Ξ_i^-, and $\mathcal{U}_i^-$ in (3.20) into the data-driven LMI (3.32) and selecting $r_i = 0.5$ for all $i = \{1, 2, \ldots, 6\}$, we can obtain a set of feasible augmented gain matrices

$$\mathcal{K}_1 = \left[\begin{array}{c|c} \mathcal{K}_1^1 & \mathcal{K}_1^2 \end{array}\right] = \left[\begin{array}{cc|c} -1.0057 & 0.4365 & -0.8872 \end{array}\right],$$
$$\mathcal{K}_2 = \left[\begin{array}{c|c} \mathcal{K}_2^1 & \mathcal{K}_2^2 \end{array}\right] = \left[\begin{array}{cc|c} -1.0996 & 0.2996 & -0.9951 \end{array}\right],$$

$$\mathcal{K}_3 = \left[\begin{array}{c|c} \mathcal{K}_3^1 & \mathcal{K}_3^2 \end{array}\right] = \left[\begin{array}{cc|c} -1.1466 & 0.9283 & -0.8499 \end{array}\right],$$
$$\mathcal{K}_4 = \left[\begin{array}{c|c} \mathcal{K}_4^1 & \mathcal{K}_4^2 \end{array}\right] = \left[\begin{array}{cc|c} -0.7249 & 0.0736 & -0.8741 \end{array}\right],$$
$$\mathcal{K}_5 = \left[\begin{array}{c|c} \mathcal{K}_5^1 & \mathcal{K}_5^2 \end{array}\right] = \left[\begin{array}{cc|c} -1.1766 & 0.0126 & -0.9634 \end{array}\right],$$
$$\mathcal{K}_6 = \left[\begin{array}{c|c} \mathcal{K}_6^1 & \mathcal{K}_6^2 \end{array}\right] = \left[\begin{array}{cc|c} -0.3805 & -0.0282 & -0.6359 \end{array}\right].$$

Based on $\mathcal{Z}_1$ and $\mathcal{Z}_2$ as well as the obtained augmented gain matrices above, we construct the distributed control protocol (3.1) and (3.2). To evaluate the effectiveness of the proposed method against the reference signal changes, the reference voltage for the six DGUs is set as

$$\begin{cases} y_r = 48V, & 0 \le t \le 1s, \\ y_r = 60V, & 1s < t \le 2s, \\ y_r = 48V, & 2s < t \le 3.5s, \\ y_r = 36V, & 3.5s < t \le 4.5s, \\ y_r = 48V, & t > 4.5s. \end{cases}$$

By utilizing the proposed control protocol and selecting the initial state $\eta_i(0) = 0$ and $x_i(0) = \left[\begin{array}{cc} 0 & 0 \end{array}\right]^{\top}$, the output voltages of the six DGUs are shown in Figure 3. It can be seen that the output voltages of the six DGUs accurately track the reference voltage y_r, even when the reference signal is changing. This indicates that the proposed methods are effective and have robustness against noise.

To verify $\mathcal{D}_Q$-stabilizable performance guarantee, we conduct a comparative experiment. The results shown in Figure 3 are obtained with $r_i = 0.5$. Next, we select $r_i = 0.9$ for all $i = \{1, 2, \ldots, 6\}$ and solve the data-driven LMI (3.32), and the feasible augmented gain matrices are given as

$$\mathcal{K}_1 = \left[\begin{array}{c|c} \mathcal{K}_1^1 & \mathcal{K}_1^2 \end{array}\right] = \left[\begin{array}{cc|c} -0.3081 & 0.4093 & -0.2748 \end{array}\right],$$
$$\mathcal{K}_2 = \left[\begin{array}{c|c} \mathcal{K}_2^1 & \mathcal{K}_2^2 \end{array}\right] = \left[\begin{array}{cc|c} -0.6198 & 0.4032 & -0.5768 \end{array}\right],$$
$$\mathcal{K}_3 = \left[\begin{array}{c|c} \mathcal{K}_3^1 & \mathcal{K}_3^2 \end{array}\right] = \left[\begin{array}{cc|c} -0.5427 & 0.8135 & -0.4093 \end{array}\right],$$
$$\mathcal{K}_4 = \left[\begin{array}{c|c} \mathcal{K}_4^1 & \mathcal{K}_4^2 \end{array}\right] = \left[\begin{array}{cc|c} -0.2404 & -0.1552 & -0.5312 \end{array}\right],$$
$$\mathcal{K}_5 = \left[\begin{array}{c|c} \mathcal{K}_5^1 & \mathcal{K}_5^2 \end{array}\right] = \left[\begin{array}{cc|c} -0.6798 & 0.0759 & -0.5002 \end{array}\right],$$
$$\mathcal{K}_6 = \left[\begin{array}{c|c} \mathcal{K}_6^1 & \mathcal{K}_6^2 \end{array}\right] = \left[\begin{array}{cc|c} -0.1188 & -0.1977 & -0.3036 \end{array}\right].$$

By substituting these gain matrices into the control protocol (3.1) and (3.2), the output voltages of the six DGUs are shown in Figure 4. It is obvious that the speed at which the output voltages of the six DGUs track the reference voltage in Figure 4 is slower than that in Figure 3. This is because a smaller r_i enables the eigenvalues of $\mathcal{A}_i + \mathcal{B}_i\mathcal{K}_i$ to be closer to the origin. This ensures that the tracking error system (3.13) has a faster convergence rate. However, a faster convergence rate requires a greater control input, which may cause the tracking error system to experience severe vibrations. Therefore, a trade-off needs to be achieved between the convergence rate and the control energy.

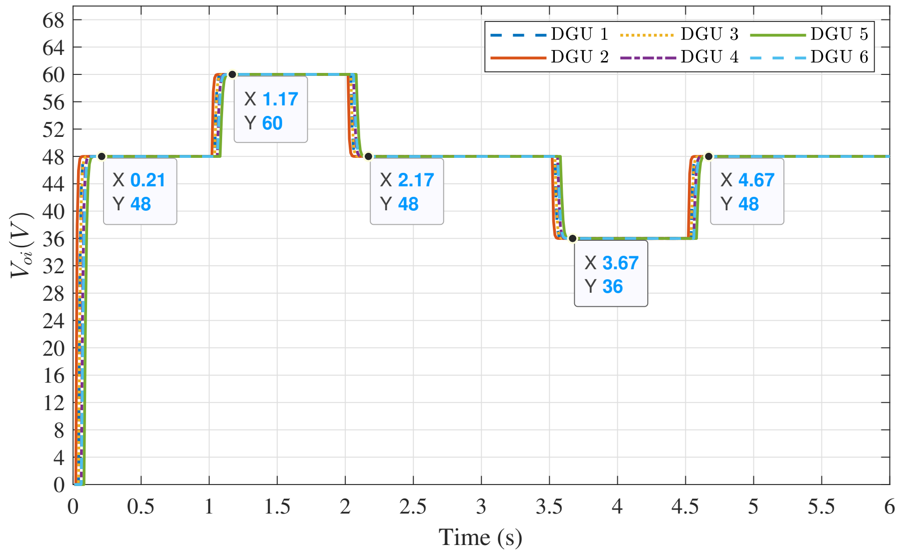

Figure 3. The output voltages of six DGUs under the gain matrices with $r_i = 0.5$.

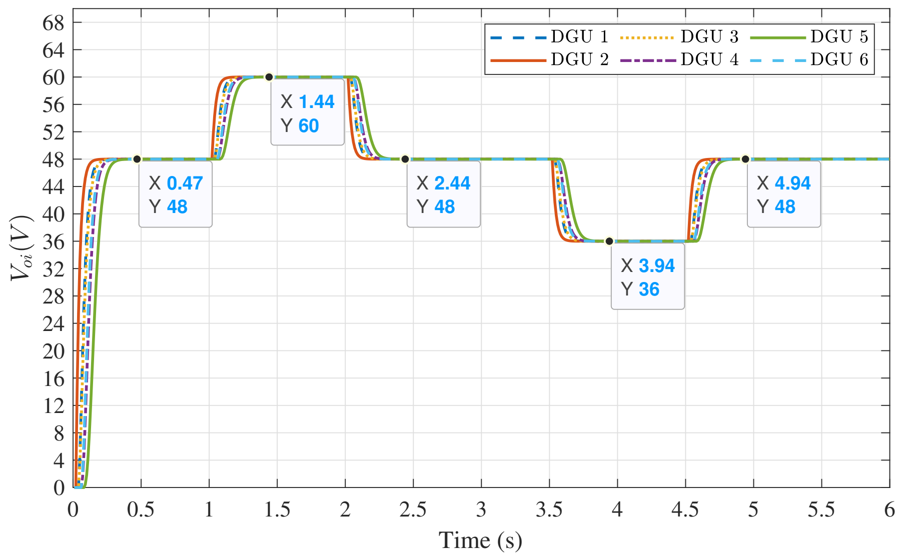

Figure 4. The output voltages of six DGUs under the gain matrices with $r_i = 0.9$.

To validate robustness, we assess the feasibility of the data-based LMI (3.32) under varying levels of measurement noise. Specifically, DGU 6 is selected for this test with $r_6 = 0.85$, and the noise intensity ϖ_6 is varied over the set $\{0.01, 0.05, 0.1, 0.15, 0.2, 0.25, 0.3\}$. The results are summarized in Table 2. As shown in Table 2, the data-driven LMI (3.32) remains feasible for noise levels $\varpi_6 \in \{0.01, 0.05, 0.1, 0.15, 0.2\}$. However, it becomes infeasible when the noise level increases to $\varpi_6 \in \{0.25, 0.3\}$. Nevertheless, the existence of a feasible gain for $\varpi_6 \leq 0.2$ demonstrates that the proposed control method exhibits robustness against moderate levels of measurement noise.

Table 2. The feasibility of the data-based LMI (3.32) for DGU 6 under different noise levels ϖ_6.

ϖ_6	0.01	0.05	0.1	0.15	0.2	0.25	0.3
Feasibility	Yes	Yes	Yes	Yes	Yes	No	No

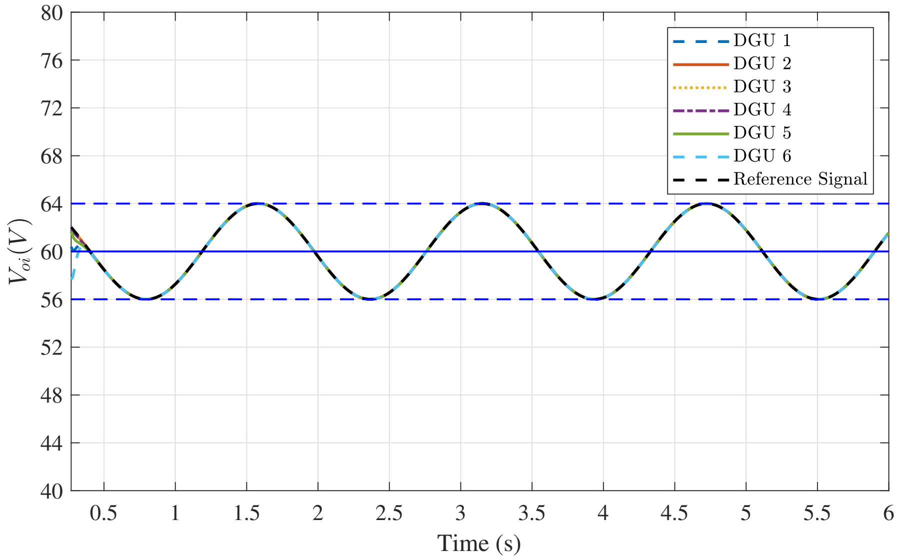

Figure 5. The output voltages of six DGUs under the gain matrices with $r_i = 0.85$.

In order to further verify that our proposed method is not only capable of tracking a constant signal as in [21, 22] but also able to track a time-varying reference signal, we select

$$D = \begin{bmatrix} 0.9992 & 0.04 & 0 \\ -0.04 & 0.9992 & 0 \\ 0 & 0 & 1 \end{bmatrix}, \; E = \begin{bmatrix} 1 & 0 & 1 \end{bmatrix},$$

and $x_r(0) = \begin{bmatrix} 4 & 0 & 60 \end{bmatrix}$. Given the D, E, and $x_r(0)$, the reference signal (2.4) can generate a sinusoidal signal with an angular frequency of 4 rad/s that fluctuates between 56 V and 64 V. According to (3.3), one has

$$\mathcal{Z}_1 = \begin{bmatrix} 0 & 1 & 0 \\ 0 & 0 & 1 \\ 1 & -2.9984 & 2.9984 \end{bmatrix}, \; \mathcal{Z}_2 = \begin{bmatrix} 0 & 0 & 1 \end{bmatrix}^{\top}.$$

As before, we can obtain a set of feasible augmented gain matrices

$$\mathcal{K}_1 = \begin{bmatrix} \mathcal{K}_1^1 \mid \mathcal{K}_1^2 \end{bmatrix} = \begin{bmatrix} -1.6882 & 0.4112 \mid -1.5218 & 3.5542 & -2.1092 \end{bmatrix},$$
$$\mathcal{K}_2 = \begin{bmatrix} \mathcal{K}_2^1 \mid \mathcal{K}_2^2 \end{bmatrix} = \begin{bmatrix} -1.4001 & 0.1291 \mid -1.2756 & 2.9105 & -1.6817 \end{bmatrix},$$
$$\mathcal{K}_3 = \begin{bmatrix} \mathcal{K}_3^1 \mid \mathcal{K}_3^2 \end{bmatrix} = \begin{bmatrix} -1.2819 & 0.7551 \mid -1.1214 & 2.5750 & -1.4940 \end{bmatrix},$$

$$\mathcal{K}_4 = \left[\begin{array}{c|c} \mathcal{K}_4^1 & \mathcal{K}_4^2 \end{array}\right] = \left[\begin{array}{cc|ccc} -0.8289 & -0.0546 & -1.0036 & 2.2809 & -1.3104 \end{array}\right],$$
$$\mathcal{K}_5 = \left[\begin{array}{c|c} \mathcal{K}_5^1 & \mathcal{K}_5^2 \end{array}\right] = \left[\begin{array}{cc|ccc} -1.3656 & -0.0846 & -1.2418 & 2.8520 & -1.6531 \end{array}\right],$$
$$\mathcal{K}_6 = \left[\begin{array}{c|c} \mathcal{K}_6^1 & \mathcal{K}_6^2 \end{array}\right] = \left[\begin{array}{cc|ccc} -1.4591 & 0.0748 & -1.6498 & 4.1104 & -2.6899 \end{array}\right].$$

Based on these results, the output voltages of the six DGUs are shown in Figure 5. It can be observed that the six DGUs can track the time-varying reference voltage y_r. Compared with [21, 22], the proposed methods ensure that all DGUs can not only track a constant signal but also track a time-varying signal. Furthermore, the feasible control protocols can be designed without any parameter information of the DGUs even in the presence of unknown noise. Although the methods proposed in [21, 22] also possess certain robustness, the precise system parameter information is required when designing the control protocol. Therefore, the proposed methods are more general and applicable.

5. Conclusions

This paper has proposed a novel data-driven robust distributed control strategy for the cooperative voltage regulation of a DC microgrid. The primary objective of ensuring that all DGUs accurately track a specified reference voltage has been successfully achieved. A key advantage of the proposed distributed control protocol over traditional decentralized approaches is that it eliminates the need for each DGU to have global knowledge of the reference signal, relying instead on communication with neighboring DGUs only. To address the practical challenges of unknown DGU parameters and measurement noises, a data-driven robust control method has been developed. The core of this approach lies in the transformation of the cooperative voltage regulation problem into a local stabilization problem. By leveraging noisy data collected from the local DGU and the constructed auxiliary system, a data-driven design procedure has been formulated to solve for the gain matrices of the controller. Crucially, the application of $\mathcal{D}_Q$-stabilization theory has enabled the formulation of a data-driven LMI, which guarantees that the closed-loop system's eigenvalues reside within a specified region in the unit disk, thus ensuring stability and robust performance of the DC microgrid. The proposed methods can only address the issue of measurement data affected by additive noise. How to design a data-driven control protocol in the presence of multiplicative noise is our future research direction.

Use of AI tools declaration

The authors declare they have not used Artificial Intelligence (AI) tools in the creation of this article.

Acknowledgments

This work was supported in part by the National Natural Science Foundation of China under Grant 62503234, and in part by the Natural Science Foundation of Jiangsu Province under Grant BK20230378.

Conflict of interest

The authors declare there are no conflicts of interest.

References

1. M. K. Senapati, O. Al Zaabi, K. Al Hosani, K. Al Jaafari, C. Pradhan, U. R. Muduli, Advancing electric vehicle charging ecosystems with intelligent control of DC microgrid stability, *IEEE Trans. Ind. Appl.*, **60** (2024), 7264–7278. https://doi.org/10.1109/TIA.2024.3413052
2. S. Fan, Y. K. Fu, Y. Liu, C. Deng, Round-robin-based cooperative resilient control for AC/DC MG under FDI attacks, *IEEE Trans. Ind. Electron.*, **17** (2025), 8419–8428. https://doi.org/10.1109/TIE.2024.3522484
3. H. Pan, X. Feng, F. Li, J. Yang, Energy coordinated control of DC microgrid integrated incorporating PV, energy storage and EV charging, *Appl. Energy*, **342** (2023), 121155. https://doi.org/10.1016/j.apenergy.2023.121155
4. C. Deng, Y. Wang, C. Wen, Y. Xu, P. Lin, Distributed resilient control for energy storage systems in cyber-physical microgrids, *IEEE Trans. Ind. Inf.*, **17** (2020), 1331–1341. https://doi.org/10.1109/TII.2020.2981549
5. H. Shen, W. Zhao, J. Cao, J. H. Park, J. Wang, Predefined-time event-triggered tracking control for nonlinear servo systems: A fuzzy weight-based reinforcement learning scheme, *IEEE Trans. Fuzzy Syst.*, **32** (2024), 4557–4569. https://doi.org/10.1109/TFUZZ.2024.3403917
6. S. Huo, G. Liu, H. Shen, C. Deng, Y. Zhang, Robust data-driven containment of fully unknown heterogeneous MASs from noisy data, *IEEE Trans. Syst. Man Cybern. Syst.*, **55** (2025), 3668–3678. https://doi.org/10.1109/TSMC.2025.3545832
7. S. Huo, Y. Zhang, F. L. Lewis, C. Sun, Observer-based resilient consensus control for heterogeneous multiagent systems against cyberattacks, *IEEE Trans. Control Netw. Syst.*, **10** (2022), 647–658. https://doi.org/10.1109/TCNS.2022.3203905
8. C. L. Bhattar, M. A. Chaudhari, Centralized energy management scheme for grid connected DC microgrid, *IEEE Syst. J.*, **17** (2023), 3741–3751. https://doi.org/10.1109/JSYST.2022.3231898
9. M. Saleh, Y. Esa, A. Mohamed, Centralized control for DC microgrid using finite state machine, in *2017 IEEE Power & Energy Society Innovative Smart Grid Technologies Conference (ISGT)*, IEE, (2017), 1–5. https://doi.org/10.1109/ISGT.2017.8086062
10. F. Guo, Z. Lian, X. Zheng, C. Deng, C. Wen, J. He, Decentralized cluster-based distributed secondary control of large-scale DC microgrid cluster system, *IEEE Trans. Sustainable Energy*, **15** (2024), 1652–1662. https://doi.org/10.1109/TSTE.2024.3365593
11. C. Weng, Y. Peng, Adaptive and decentralized control strategy to support coordination of multiple DC microgrids considering transmission line impedance, *IEEE Trans. Smart Grid*, **16** (2025), 2026–2039. https://doi.org/10.1109/TSG.2025.3536159
12. Z. Li, B. Wang, L. Xian, M. Zhang, Q. Xu, Decentralized active disturbance rejection control for hybrid energy storage system in DC microgrid, *IEEE Trans. Ind. Electron.*, **71** (2024), 14232–14243. https://doi.org/10.1109/TIE.2024.3363772

13. Z. Fan, B. Fan, W. Liu, Distributed control of DC microgrids for optimal coordination of conventional and renewable generators, *IEEE Trans. Smart Grid*, **12** (2021), 4607–4615. https://doi.org/10.1109/TSG.2021.3094878

14. B. Fan, J. Peng, Q. Yang, W. Liu, Distributed control of DC microgrids with improved ZIP load adaptability, *IEEE Trans. Syst. Man Cybern. Syst.*, **52** (2021), 4623–4633. https://doi.org/10.1109/TSMC.2021.3101813

15. M. S. Sadabadi, A resilient-by-design distributed control framework for cyber-physical DC microgrids, *IEEE Trans. Control Syst. Technol.*, **32** (2023), 625–636. https://doi.org/10.1109/TCST.2023.3324530

16. J. Zhou, Q. Yang, X. Chen, Y. Chen, J. Wen, Resilient distributed control against destabilization attacks in DC microgrids, *IEEE Trans. Power Syst.*, **38** (2023), 371–384. https://doi.org/10.1109/TPWRS.2022.3164398

17. Y. Huang, G. P. Liu, Y. Yu, W. Hu, Data-driven distributed predictive control for voltage regulation and current sharing in DC microgrids with communication constraints, *IEEE Trans. Cybern.*, **54** (2024), 4998–5011. https://doi.org/10.1109/TCYB.2024.3372616

18. X. Dong, H. Zhang, X. Xie, Z. Ming, Data-driven distributed H_∞ current sharing consensus optimal control of DC microgrids via reinforcement learning, *IEEE Trans. Circuits Syst. I Regul. Pap.*, **71** (2024), 2824–2834. https://doi.org/10.1109/TCSI.2024.3366942

19. A. S. Soliman, M. M. Amin, F. F. M. El-Sousy, O. A. Mohammad, Experimental validation for artificial data-driven tracking control for enhanced three-phase grid-connected boost rectifier in DC microgrids, *IEEE Trans. Ind. Appl.*, **59** (2022), 2563–2580. https://doi.org/10.1109/TIA.2022.3227137

20. H. Zhang, J. Zhou, Q. Sun, J. M. Guerrero, D. Ma, Data-driven control for interlinked AC/DC microgrids via model-free adaptive control and dual-droop control, *IEEE Trans. Smart Grid*, **8** (2015), 557–571. https://doi.org/10.1109/TSG.2015.2500269

21. S. Derakhshan, M. Shafiee-Rad, Q. Shafiee, M. R. Jahed-Motlagh, Decentralized robust LMI-based voltage control strategy for autonomous inverter-interfaced multi-DG microgrids, *IEEE Trans. Power Syst.*, **38** (2022), 3003–3015. https://doi.org/10.1109/TPWRS.2022.3204625

22. M. S. Sadabadi, Q. Shafiee, A. Karimi, Plug-and-play robust voltage control of DC microgrids, *IEEE Trans. Smart Grid*, **9** (2017), 6886–6896. https://doi.org/10.1109/TSG.2017.2728319

23. J. Huang, *Nonlinear Output Regulation: Theory and Applications*, SIAM, 2004. https://doi.org/10.1137/1.9780898718683

24. S. Huo, Z. Wang, H. Shen, Y. Zhang, C. Deng, Data-based output containment of completely heterogeneous multi-agent systems with unknown dynamics and its application, *IEEE Trans. Circuits Syst. I Regul. Pap.*, **72** (2025), 2903–2914. https://doi.org/10.1109/TCSI.2025.3547894

25. J. Huang, The cooperative output regulation problem of discrete-time linear multi-agent systems by the adaptive distributed observer, *IEEE Trans. Autom. Control*, **62** (2016), 1979–1984. https://doi.org/10.1109/TAC.2016.2592802

26. H. Ye, C. Wen, Y. Song, Decentralized and distributed control of large-scale interconnected multi-agent systems in prescribed time, *IEEE Trans. Autom. Control*, **70** (2024), 1115–1130. https://doi.org/10.1109/TAC.2024.3451213

27. D. Peaucelle, D. Arzelier, O. Bachelier, J. Bernussou, A new robust D-stability condition for real convex polytopic uncertainty, *Syst. Control Lett.*, **40** (2000), 21–30. https://doi.org/10.1016/S0167-6911(99)00119-X

28. H. J. van Waarde, M. K. Camlibel, M. Mesbahi, From noisy data to feedback controllers: Nonconservative design via a matrix S-lemma, *IEEE Trans. Autom. Control*, **67** (2020), 162–175. https://doi.org/10.1109/TAC.2020.3047577

29. H. Ye, C. Wen, Y. Song, Distributed matrix pencil formulations for prescribed-time leader-following consensus of MASs with unknown sensor sensitivity, *IEEE Trans. Syst. Man Cybern. Syst.*, **56** (2026), 629–641. https://doi.org/10.1109/TSMC.2025.3627671

AIMS Press